Nanoscale

PAPER

View Article Online
View Journal

Cite this: DOI: 10.1039/d6nr00599c

Cellulose nanocrystal gels as radical reservoirs

Jiaou Ren, [a] Yota Neagari, [a] Yihan Shi,[a] Zongzhe Li, [a] Lucas J. Andrew, [a] Miguel A. Soto *[a,b] and Mark J. MacLachlan *[a,c,d]

Received 11th February 2026,
Accepted 6th May 2026

DOI: 10.1039/d6nr00599c

rsc.li/nanoscale

Gels that sustain reactive radical species under aerobic ambient conditions remain rare, limiting the development of soft materials that exploit redox-active chemistry. Here, we show that cellulose nanocrystal (CNC) gels containing a deep eutectic solvent (DES) create an oxygen-resistant environment that supports the photochemical and electrochemical generation of long-lived viologen radicals. The DES medium drives gel formation and produces mechanically strong networks in which viologen radical formation is fully reversible and coupled to optical and mechanical responses. These gels function as redox-responsive media for information storage, enabling photoactive and electroactive coatings with spatial and temporal control over message development. Extending the platform to a tetracationic viologen macrocycle shows that radical–radical host–guest complexes can form and dissociate within the gel matrix, giving rise to an optical response distinct from those of the individual radicals. These results establish DES-containing CNC gels as a versatile platform for stabilizing and manipulating radical species in soft materials, opening new avenues to aerobic electrochromic devices, UV-responsive systems, and in-gel supramolecular redox chemistry.

Introduction

Gels are common in everyday life,[1] but also have applications that extend well beyond the familiar.[2–6] For example, they play important roles in advanced technologies ranging from smart flexible electronics[7] to 3D printing[8] and therapeutics.[9] Their design space is remarkably broad, as diverse scaffolds can be incorporated into gel networks to impart targeted functions and properties.[10–12]

Gels contain entangled networks that entrap large volumes of solvent relative to the network mass. While many are stabilized by covalent crosslinks,[13] others rely partly or entirely on non-covalent interactions,[14] imparting features such as reversibility, environmental responsiveness, and recyclability. In our group, we design non-covalent gels by employing cellulose nanocrystals (CNCs) as nanostructured scaffolds.[15–18]

A particular type of CNCs is obtained by acidic digestion of cellulose in aqueous H_2SO_4. This process removes the amorphous domains in naturally occurring cellulose and leaves behind CNCs as crystalline, rod-like nanoparticles.[19] During this treatment, sulfate half-ester groups are installed on the CNC's surface, imparting negative charge and stabilizing aqueous suspensions through inter-particle electrostatic repulsion.[20] Addition of salts to a CNC suspension screens the nanorods' charges, and beyond a critical salt concentration, the particles aggregate to form gels (Fig. 1a).[21–25] We have used this ion-aided strategy to incorporate functional ionic species that not only facilitate gelation but also perform secondary roles, such as guest capture through inclusion complexes.[26,27] This modular approach provides a robust platform for designing adaptive materials.[28,29]

Here, we report CNC-based gels that incorporate radical-forming species that can be photo- and electroactivated to generate long-lived radical cations *in situ* under aerobic conditions. These materials are made from CNC scaffolds, an ionic medium that promotes gelation, and a class of redox-active molecules known as viologens.

Paraquat (**1**, Fig. 1b), a canonical alkyl viologen, undergoes a well-established two-step reduction, with the first electron transfer producing a blue–violet radical cation (**2**).[30] The reversible redox chemistry and distinct photophysical changes of viologens[31,32] have facilitated their widespread use in today's materials landscape, including organic batteries,[33] smart coatings,[34] and other advanced devices.[35–37]

Viologens have been incorporated on supporting scaffolds[38,39] including biomacromolecules,[40] synthetic polymers,[41,42] and reticular frameworks.[43] These systems show reversible redox activity and can generate the corresponding radical species upon electro- and photo-stimulation. However, their operation typically requires anaerobic conditions to prevent rapid oxidation of the radicals back to the cationic

[a]*Department of Chemistry, University of British Columbia, 2036 Main Mall, Vancouver, British Columbia V6T 1Z1, Canada. E-mail: mmaclach@chem.ubc.ca*
[b]*Department of Chemistry, University of Saskatchewan, 110 Science Place, Saskatoon, Saskatchewan S7N 5C9, Canada*
[c]*Quantum Matter Institute, University of British Columbia, 2355 East Mall, Vancouver, BC, V6T 1Z4 Canada*
[d]*WPI Nano Life Science Institute, Kanazawa University, Kanazawa, 920-1192 Japan*

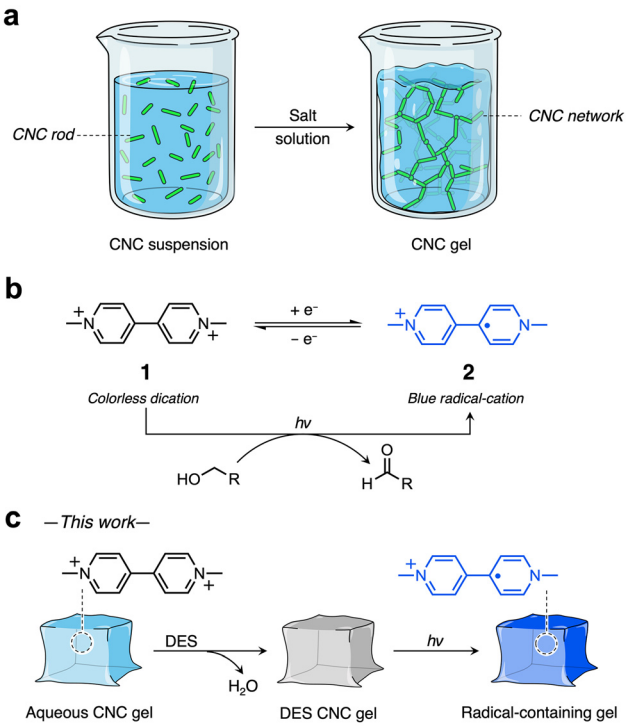

Fig. 1 (a) Cartoon representation of the ion-induced gelation of aqueous CNCs *via* particle aggregation. (b) Electro- and photochemical reduction of the paraquat dication (**1**) to its radical cation (**2**). (c) Schematic overview of this work: fabrication of CNC–viologen gels containing a deep eutectic solvent (DES) as the continuous medium that promotes photoreduction and stabilizes the resulting viologen radicals.

state. Materials capable of stabilizing viologen radicals under ambient aerobic conditions remain scarce.[44–47]

In previous work from our group, we demonstrated that CNC-paraquat films function as photo- and redox-active materials that form radicals even under aerobic conditions.[47] To the best of our knowledge, however, gel materials have not yet succeeded in stabilizing pure paraquat radicals under such aerobic conditions. Achieving this would represent a significant advance, with potential applications in spintronics,[48] in-gel radical catalysis, and ferromagnetic materials,[49] eliminating the need for rigorously deoxygenated conditions.

Paraquat radicals are typically short-lived in oxygenated media, where dissolved O_2 either prevents their formation or rapidly quenches them. Recently, the Scherman group[46] demonstrated that deep eutectic solvents (DESs) facilitate viologen reduction. Reports suggest that process proceeds through a photoinduced electron transfer from the counterion (typically Cl^-) to the ground-state viologen, yielding the corresponding radical cation (Fig. 1b).[50] The resulting radicals are surprisingly stable, due to the low oxygen permeability of DES.[51] Building on this, we hypothesized that combining DES, viologens, and CNCs could yield robust photo- and electroactive gels capable of generating stable radical-containing networks (Fig. 1c). Such gels would not only be safer to handle than viologen–DES solutions, but could also be readily shaped or patterned, facilitating their integration into electrochromic devices, coatings, and other functional platforms.

Results and discussion

We first investigated the gelation of CNCs in the presence of DES (choline chloride/glycerol). Addition of DES (200 μL) to an aqueous CNC dispersion (1.8 mL, 5 wt%, pH 5.3, $\zeta = -60$ mV) resulted in fast (<1 min) gel formation (see preparation details in SI (Table S1)). ζ-Potential measurements showed that increasing the DES content (0.6 to 10 vol%) changes the apparent surface charge of CNCs from −52 mV to −7 mV (Fig. 2a and Fig. S1), consistent with electrostatic screening of interparticle repulsion – the key driving force for CNC gelation. Rheological analysis showed that the complex modulus (G^*) at an oscillatory frequency (ω) of 10 rad s^{-1} increases with DES concentration, from 41 Pa to 303 Pa in the 0.6–5.0 vol% range (Fig. 2b), demonstrating that higher gelator content yields mechanically stiffer materials (see G', G'', and G^* in Fig. S2–S5). These gels showed no visible change in optical properties after photoirradiation at 302 nm for 10 min.

We next introduced paraquat (**1**, Cl^- salt) into the DES medium (50 mM) and added different amounts of this mixture (0.6 to 10 vol%) to aqueous CNC dispersions (see Table S2 for details). Gelation occurred in all samples. ζ-Potential values (from −32 mV to −9.5 mV, Fig. 2a and Fig. S6) and G^* measurements confirmed that both electrostatic double-layer compression and mechanical stiffness can be tuned by the amount of **1** in DES added to the system. For example, at ω = 10 rad s^{-1}, G^* increases from 40 Pa at 1.25 vol% of the DES–**1** gelator to 682 Pa at 5 vol% (Fig. 2b and Fig. S7–S10). At low concentrations of **1**, the mechanical response is nearly unchanged compared with gels prepared using DES alone (40 Pa for DES–**1** *vs.* 41 Pa for DES only). However, at higher concentrations, *e.g.* 5 vol%, the gel containing **1** becomes roughly 125% stiffer than the DES-only material. This trend is consistent with the increased ionic strength of the medium, which enhances interparticle aggregation.

Despite the presence of the redox-active compound **1** and DES in the materials, photoirradiation at 302 nm for 10 min,

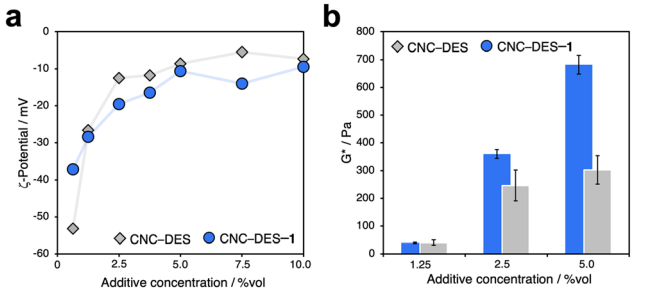

Fig. 2 (a) ζ-Potential and (b) G^* values (ω = 10 rad s^{-1}) for CNC gels prepared with varying concentrations of CNC–DES or CNC–DES–**1** solution. Error bars represent standard deviations from three independent measurements.

did not produce any visible change. We attributed this lack of response to the high-water content in the gels (90–98 vol% of the medium, Table S2), which is typically saturated with air, thus preventing radical formation. To address this, we performed solvent exchange on a robust gel formulation (composition: aqueous CNCs (1.8 mL, 5 wt%) and DES-**1** (200 μL, 50 mM solution)). After setting, the gel was immersed in DES (15 mL) for 8 h, the supernatant was removed and replaced with fresh DES (15 mL). The system was then left to equilibrate for 8 h. This process was repeated once more to complete three concurrent solvent exchange processes (full preparation details in SI). Using this method, we prepared three independent DES-saturated gels. The material (CNC–DES–**1**) remained colorless but was noticeably tougher to the touch than those containing mostly water as the continuum. Rotational rheology confirmed this observation with a G^* larger (5412 Pa at ω = 10 rad s^{-1}) than that of water-containing analogues (682 Pa at ω = 10 rad s^{-1}, Fig. S11). We attributed this stiffening to enhanced interparticle interactions within the highly ionic DES medium, which more effectively screens CNC–CNC electrostatic repulsion.[52]

Upon photoirradiation at 302 nm for 10 min, the material CNC–DES–**1** turned deep blue (Fig. 3a), consistent with the formation of radical cation **2** within the gel matrix.[53] Photoreduction of paraquat is generally understood to proceed through photoinduced electron transfer pathways involving either the Cl^- counterion or hydroxyl-containing species, the latter being concomitantly oxidized to the corresponding aldehydes or ketones.[54,55] In the present system, both pathways are likely happening, given the high concentration of Cl^- (from DES and **1**) and hydroxyl groups (from DES and CNCs) within the gel. Notably, control experiments using DES-free hydrogels showed no detectable photoreduction under identical conditions.

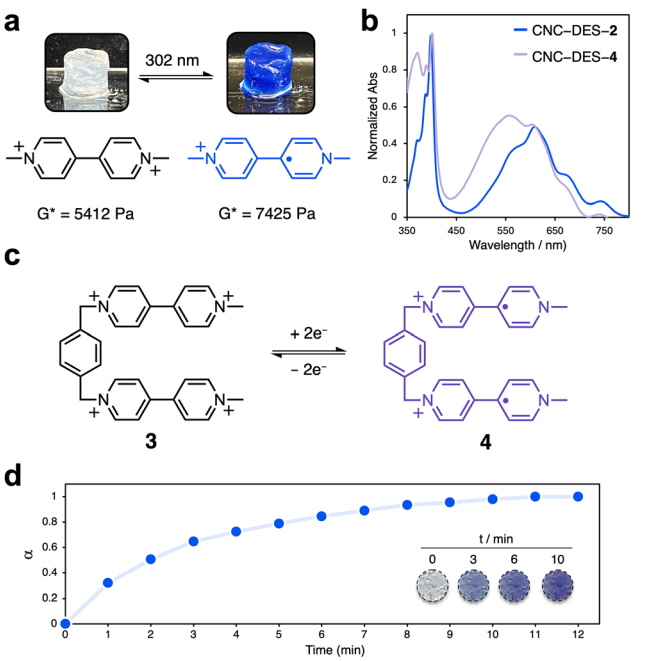

Fig. 3 (a) Photoreduction of CNC–DES–**1** at 302 nm. Each gel is approximately 1 cm^3. (b) UV-vis spectra of CNC–DES–**2** and CNC–DES–**4** obtained after photoirradiation of the corresponding di- and tetracationic precursors. (c) Chemical structures of tetracation **3** and its diradical dication **4** formed upon two-electron reduction. (d) Fractional color development (α) of CNC–DES–**3** during photoreduction under sunlight; insets show the progression at the indicated irradiation times. $\alpha = (I_0 - I_f)/(I_0 - I_t)$; I_0 = initial color intensity; I_f = final color intensity; I_t = color intensity at time t (see SI for details).

The UV-vis spectrum of the photoirradiated gel matched that of **2** in DES solution (Fig. S12), with a charge-transfer (CT) band centered at ~610 nm (Fig. 3b), confirming the reduction of **1** to **2** within the gel. Remarkably, the blue color persisted for 12 h in air, both under ambient light and in the dark. Even after cutting a gel to expose the fresh interior, the bulk remained intensely blue, highlighting the long-lived character of the radicals. Notably, decolorization was initially observed only at the air interface, while the interior of the material retained its color, indicating that oxygen gradually permeates the gel and quenches the radical species.

To quantify this process, time-dependent UV-vis measurements were performed by monitoring the decay of the CT band at 610 nm. For a thin film of CNC–DES–**2** (~2 mm thickness), the radical species decayed to the oxidized form within approximately 100 min after exposure to air (Fig. S13). In bulk samples, oxidation proceeded significantly more slowly, with complete return to the colorless state only after 24 h in air (dark). The process could be accelerated by crushing and vigorously stirring the material, which facilitates air penetration into the matrix.

The high stability of the radical species within the gel can be attributed to a combination of factors, including the reduced oxygen permeability of the DES medium[56] and the presence of hydroxyl-rich components, which are known to promote rapid quenching of the viologen excited state and facilitate radical formation.[56] The redox process was reversible over five consecutive cycles (Fig. S14) without detectable residual radicals (Fig. S15).

Considering that the mechanical properties of CNC gels depend strongly on ion content, we hypothesized that reducing dication **1** to radical cation **2** would alter gel stiffness. Rheology confirmed this effect: at ω = 10 rad s^{-1}, G^* increased by 37% upon photoreduction, from 5.4 kPa to 7.4 kPa, in line with a lower electrostatic repulsion in the radical-containing gel (CNC–DES–**2**). The observed increase in gel robustness likely arises from a combination of inter-radical interactions,[57,58] that reinforce the gel network and changes in ionic strength, as well as network restructuring independent of radical interactions. The stiffening is transient, and oxidation partially restores the viscoelastic properties of the material (G^* = 6.2 kPa, Fig. S16). The change in viscoelastic properties is accompanied by a visible optical response, where color formation indicates stiffening and its loss implies softening.

We next explored the scope of our design by testing other viologens. Initially, we studied the tetracation **3** (Fig. 3c), which undergoes a two-electron reduction to give the intensely

colored diradical dication **4**.[59] The corresponding gel was prepared following the same procedure established for **1** and subsequently subjected to solvent exchange (water to DES), rendering CNC–DES–**3** (see Table S3). Upon irradiation at 302 nm, the material turned purple, consistent with formation of the corresponding diradical dication **4**. The UV-vis spectrum of the material closely resembled that obtained for the CNC gel containing **2**, but with a characteristic red shift (Fig. 3b), as expected for species bearing two viologen units in their structures.[60]

CNC–DES–**3** gels also undergo photoreduction when exposed to natural light (SI Video S1, gelator concentration 5 vol%, Table S3). Under sunlight, the gel gradually turned blue within 5 min at a UV index of 5 and T of 25 °C. The color change followed a consistent trend (Fig. 3d) and reached completion after approximately 10 min. This response shows the potential of CNC–DES–**3** for UV-dosimetry applications, as color development can be correlated with UV-light exposure time. As observed for irradiation at 302 nm, the gels recovered their original, colorless state when kept in the dark at room temperature.

In designing these materials, we were particularly interested in evaluating their applications. As a proof-of-concept, we focused on two directions: photoactive and electroactive coatings, and in-gel, light-controlled host–guest assembly and disassembly.

The first approach involves using the photoactive gels as information carriers embedded within photo-inactive masking materials. The gel CNC-DES (viologen free – aqueous CNCs (5 wt%, 1.8 mL), DES (200 μL), solvent-exchanged) was used to coat a glass substrate, while CNC–DES–**3** (aqueous CNCs (5 wt%, 1.8 mL), DES–**3** (200 μL, 25 mM), solvent-exchanged) was used to imprint a message on top of the background. Initially, the system appeared uniform and there was no message visible. Upon irradiation (302 nm), viologen **3** was reduced to purple **4**, revealing the message '*UBC*' (Fig. 4a). This process was fully reversible, and the material recovered its original uniform appearance after being kept in the dark.

Taking advantage of the electroactive responses of viologens in eutectic electrolytes,[61] we used our CNC–DES gels to make redox-active displays (Fig. S17). We first confirmed that applying a negative potential (−2.5 V) to CNC–DES–**1** sandwiched between two ITO electrodes produces a reversible color change: the initially colorless gel turns blue, displaying a CT at 604 nm in the UV-vis spectrum (Fig. S18), consistent with the reduction of **1** to **2**. The gel reached full coloration within 120 s and returned to its original state upon removal of the potential. After 180 redox cycles, the material maintained excellent color fidelity (Fig. S19).

With this established, we next fabricated an electroactive display (see Fig. 4b and Fig. S20). As shown in Fig. 4c, the message is initially invisible but becomes readable upon reduction, revealing a '*UBC*' pattern. The letters *U* and *C* are made of CNC–DES–**1**, while the letter *B* is made from CNC–DES–**3**, producing blue and purple colors, respectively (SI Video S2). This enables built-in color contrast within a single information-bearing display.

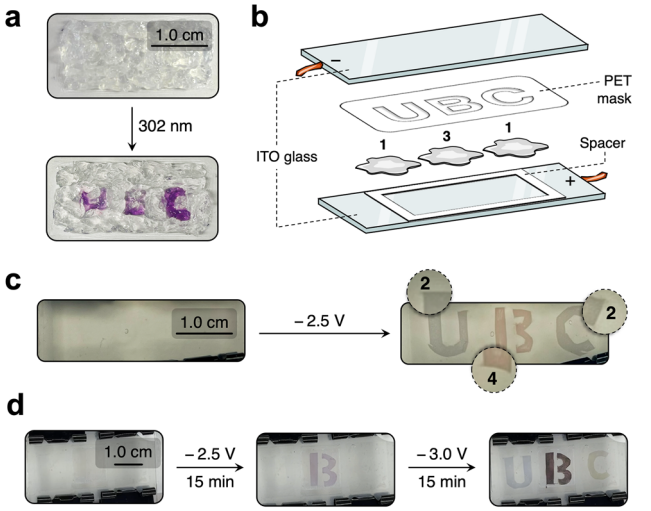

Fig. 4 (a) Two-dimensional encryption device fabricated using CNC–DES–**3** as the photoactive layer and CNC–DES as the background. (b) Cartoon representation of the assembly used for electroactive displays incorporating CNC–DES–**1** and CNC–DES–**3** as electrochromic components. (c) Electroactive display showing multicolor generation. (d) Electroactive display demonstrating spatiotemporal control over message development.

Recently, we reported electroactive CNC photonic films containing covalently attached viologens.[62] These films showed rapid color changes (~10 min), faster than the responses observed in the gels described here. We envisioned that combining both materials in a single electroactive display would allow spatiotemporal control over how a hidden message is revealed. Using a layout similar to that in Fig. 4b, we placed a CNC–viologen film in the center[62] and flanked it with two pattern carriers made from CNC–DES–**1** and CNC–DES–**3**. When a potential of −3.0 V was applied for 15 min, only the central section of the message (*B*) appeared in purple. Maintaining the potential for another 15 min revealed the side letters *U* and *C* in blue and purple, respectively (Fig. 4d). This sequential color development (SI Video S3) demonstrates how mixed CNC-based materials can be engineered to control the timing and order in which encrypted information becomes visible.

Finally, while exploring the scope of viologens compatible with our approach, we also studied the tetracationic macrocycle cyclobis(paraquat-*p*-phenylene) (**5**),[63] which undergoes a two-electron reduction to give the intensely colored diradical dication **6** (Fig. 5a).[64] In its reduced form, the macrocycle can host radical cations (*e.g.* **2**) in its cavity. The host–guest chemistry of **6** and **2**, and related radical cations, has been extensively reported in solution,[65–69] and we envisioned that an in-gel, light-controlled host–guest could be accessed. To test this, we prepared a CNC–DES gel containing equimolar amounts of dication **1** and macrocycle **5**. Following gel preparation (see Table S3), we irradiated the material at 302 nm for 10 min. This led to a color change from colorless to magenta (Fig. 5b). Notably, this color did not match that observed individually

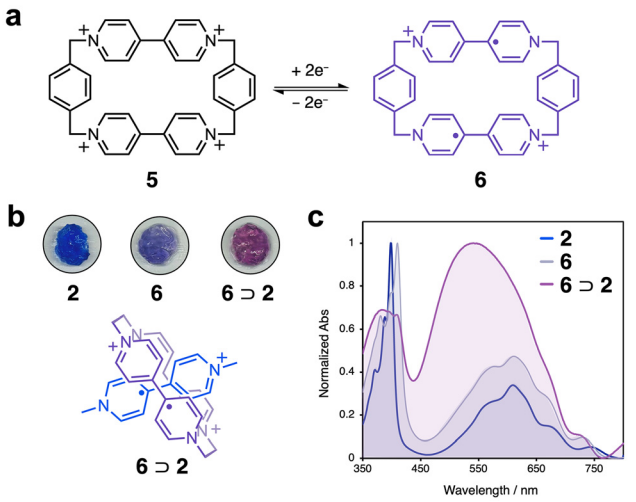

Fig. 5 (a) Chemical structures of macrocycle **5** and its radical cation **6**. (b) Photographs of CNC–DES–**2**, CNC–DES–**6**, and CNC–DES–**2**/**6** gels; the inter-radical host–guest complex formed between **2** and **6** is shown in the inset. (c) UV-vis spectra of CNC–DES–**2**, CNC–DES–**6**, and CNC–DES–**2**/**6** gels obtained after photoirradiation at 302 nm.

for radical cations **2** (blue) or **6** (purple), providing the first indication of in-gel radical–radical self-assembly.

The UV-vis spectrum of the material did not match those collected for gels containing **2** or **6** independently. Instead, the spectrum showed a red shift with an intense CT band centered at 550 nm (Fig. 5c and Fig. S21–S23). This agrees with literature reports of the in-solution host–guest complex formed between **2** and **6**, including a characteristic absorption band centered at 1100 nm, which is diagnostic of inter-radical charge transfer within the complex (Fig. S24).[65] After recovery in the dark for 22 h, the gel returned to its original colorless state (Fig. S25), showing not only the oxidation of the radical cations back to their fully cationic forms but also their dissociation into monomeric species within the gel matrix.

Conclusions

We have shown that CNCs can be assembled into robust, redox-active materials through the incorporation of viologens and deep eutectic solvents. The use of a DES in the gels allows the viologens to form long-lived radicals under ambient aerobic conditions. These radical-containing gels show stable optical responses, have reversible photo- and electro-activity, and display tunable mechanical properties that respond to the redox state of the embedded species. The combination of CNCs and DES media provides a mechanically reinforced and air-tolerant system in which the redox chemistry of viologens can be harnessed in practical forms. These properties have been used to create photoactive and electroactive coatings that store and reveal information through controlled color changes. Mixed CNC-based materials allow spatiotemporal control of redox activation, enabling decryption of messages in sequence under applied potential. By extending the platform to a viologen-based macrocycle, we demonstrated that gels can also facilitate *in situ* radical–radical host–guest chemistry, producing optical responses distinct from those of isolated radical cations and allowing reversible assembly and disassembly within a gel network.

This work establishes DES-containing CNC gels as a versatile platform for activating, stabilizing, and manipulating viologen radicals in solid-like media. The combination of redox responsiveness, mechanical tunability, and host–guest responsiveness opens new opportunities for gel-based electrochromic devices, UV-dosimetry, data encryption, in-gel supramolecular assembly, and other functional applications where redox control under ambient aerobic conditions is essential.

Author contributions

JR performed most of the experimental work. YS contributed to synthesis, YN performed electrochemical measurements, and ZL and LA supported rheological measurements. MAS conceived the concept, curated data, and wrote the first draft. MAS, JR, YS, YN and MJM contributed to manuscript writing and editing. MJM and MAS supervised the project. MJM provided funding and administered the project. All authors reviewed and approved the final manuscript.

Conflicts of interest

There are no conflicts to declare.

Data availability

All experimental procedures, characterisation data, supporting spectra, and other data can be found in the article or in the supplementary information (SI). Supplementary information is available. See DOI: https://doi.org/10.1039/d6nr00599c.

Acknowledgements

The authors thank Wadood Hamad for providing the cellulose nanocrystals used in this work. All authors also thank Saeid Kamal and Zhicheng (Paul) Xia for helpful discussions and experimental suggestions. ZL thanks UBC 4YF and MJM is grateful to NSERC for a Discovery Grant (RGPIN-2017-04899) for funding this research. MJM thanks the Canada Research Chair Program for support. MJM acknowledges the Canada Foundation for Innovation (CFI) and British Columbia Knowledge Development Fund (BCKDF) for infrastructure grants (JELF 34098, 38963). LJA thanks NSERC for a PGSD scholarship.

References

1 M. Djabourov, in *NMR and MRI of Gels*, ed. Y. De Deene, The Royal Society of Chemistry, 2020, p. 1.
2 S. Correa, A. K. Grosskopf, H. Lopez Hernandez, D. Chan, A. C. Yu, L. M. Stapleton and E. A. Appel, *Chem. Rev.*, 2021, **121**, 11385–11457.
3 A. R. Kirtane, C. Karavasili, A. Wahane, D. Freitas, K. Booz, D. T. H. Le, T. Hua, S. Scala, A. Lopes, K. Hess, J. Collins, S. Tamang, K. Ishida, J. L. P. Kuosmanen, N. U. Rajesh, N. V. Phan, J. Li, A. Krogmann, J. K. Lennerz, A. Hayward, R. Langer and G. Traverso, *Sci. Adv.*, 2022, **8**, eabm8478.
4 P. Slavík, B. R. Trowse, P. O'Brien and D. K. Smith, *Nat. Chem.*, 2023, **15**, 319–325.
5 A. López-Díaz, A. S. Vázquez and E. Vázquez, *ACS Nano*, 2024, **18**, 20817–20826.
6 X. Jiang and L. Zhou, *npj Sci. Food*, 2025, **9**, 155.
7 Y. Fang, Z. Bai, W. Xu, X. Xiong, J. Wei, Q. Hu, H. Wang and J. Cui, *Adv. Funct. Mater.*, 2025, **35**, 2416398.
8 Z. Lin, X. Qiu, Z. Cai, J. Li, Y. Zhao, X. Lin, J. Zhang, X. Hu and H. Bai, *Nat. Commun.*, 2024, **15**, 4806.
9 S. Bianco, M. Hasan, A. Ahmad, S.-J. Richards, B. Dietrich, M. Wallace, Q. Tang, A. J. Smith, M. I. Gibson and D. J. Adams, *Nature*, 2024, **631**, 544–548.
10 F. Horkay and J. F. Douglas, in *Gels and Other Soft Amorphous Solids*, American Chemical Society, 2018, vol. 1296, pp. 1–13.
11 S. Ida, T. Okuno, M. Morimura, K. Suzuki, H. Takeshita, M. Oyama, K. Nakajima and S. Kanaoka, *Polym. Chem.*, 2022, **13**, 3479–3488.
12 N. Itaya, C. Norioka, K. Satoh, M. Kamigaito, A. Kawamura and T. Miyata, *Polym. J.*, 2025, **57**, 455–466.
13 C. Xu, Y. Chen, S. Zhao, D. Li, X. Tang, H. Zhang, J. Huang, Z. Guo and W. Liu, *Chem. Rev.*, 2024, **124**, 10435–10508.
14 C. D. Jones, L. J. Kershaw Cook, A. G. Slater, D. S. Yufit and J. W. Steed, *Chem. Mater.*, 2024, **36**, 2799–2809.
15 L. Lewis, M. Derakhshandeh, S. G. Hatzikiriakos, W. Y. Hamad and M. J. MacLachlan, *Biomacromolecules*, 2016, **17**, 2747–2754.
16 A.-L. Oechsle, L. Lewis, W. Y. Hamad, S. G. Hatzikiriakos and M. J. MacLachlan, *Chem. Mater.*, 2018, **30**, 376–385.
17 L. Lewis, S. G. Hatzikiriakos, W. Y. Hamad and M. J. MacLachlan, *ACS Macro Lett.*, 2019, **8**, 486–491.
18 Z. Li, M. A. Soto, J. G. Drummond, D. M. Martinez, W. Y. Hamad and M. J. MacLachlan, *ACS Appl. Mater. Interfaces*, 2023, **15**, 8406–8414.
19 Y. Habibi, *Chem. Soc. Rev.*, 2014, **43**, 1519–1542.
20 X. M. Dong, J.-F. Revol and D. G. Gray, *Cellulose*, 1998, **5**, 19–32.
21 H. Dong, J. F. Snyder, K. S. Williams and J. W. Andzelm, *Biomacromolecules*, 2013, **14**, 3338–3345.
22 M. Chau, S. E. Sriskandha, D. Pichugin, H. Thérien-Aubin, D. Nykypanchuk, G. Chauve, M. Méthot, J. Bouchard, O. Gang and E. Kumacheva, *Biomacromolecules*, 2015, **16**, 2455–2462.
23 P. Bertsch, S. Isabettini and P. Fischer, *Biomacromolecules*, 2017, **18**, 4060–4066.
24 S. Lombardo, A. Gençer, C. Schütz, J. Van Rie, S. Eyley and W. Thielemans, *Biomacromolecules*, 2019, **20**, 3181–3190.
25 B. Motloung, R. Pfukwa and B. Klumperman, *Macromol. Mater. Eng.*, 2024, **309**, 2300457.
26 D. Zhang, M. A. Soto, L. Lewis, W. Y. Hamad and M. J. MacLachlan, *Angew. Chem., Int. Ed.*, 2020, **59**, 4705–4710.
27 Y. Shi, M. A. Soto and M. J. MacLachlan, *ACS Appl. Nano Mater.*, 2022, **5**, 17819–17827.
28 M. A. Soto, D. Zhang, Y. Xu, Y. Shi, B. O. Patrick, W. Y. Hamad and M. J. MacLachlan, *Mater. Adv.*, 2020, **1**, 2536–2541.
29 Y. Shi, R. Plavan, M. A. Soto and M. J. MacLachlan, *ChemPlusChem*, 2025, **90**, e202500453.
30 R. Rajaram and L. Neelakantan, *Results Chem.*, 2023, **5**, 100703.
31 M. Kathiresan, B. Ambrose, N. Angulakshmi, D. E. Mathew, D. Sujatha and A. M. Stephan, *J. Mater. Chem. A*, 2021, **9**, 27215–27233.
32 L. Striepe and T. Baumgartner, *Chem. – Eur. J.*, 2017, **23**, 16924–16940.
33 A. Debiais, C. Lai, T. Boulanger, G. Reynard, L. Hamlet, S. Généreux, M. Vaillancourt, R. Iftimie, H. Lebel and D. Rochefort, *ACS Appl. Energy Mater.*, 2025, **8**, 181–193.
34 H. Miao, L. Chen, F. Xing, H. Li, T. Baumgartner and X. He, *Chem. Sci.*, 2024, **15**, 7576–7585.
35 Y. Zhuang, M. Zhu, Q. Zhang, S. Ma, X. Ren, S. Wang, S. Liu and Q. Zhao, *Adv. Mater. Technol.*, 2024, **9**, 2302080.
36 J. R. Otaegui, S. Mena, J. M. Dorsainvil, G. Guirado, D. Ruiz-Molina, J. Hernando, J. C. Barnes and C. Roscini, *Chem. Mater.*, 2025, **37**, 2220–2229.
37 W. Yong, W. Liu, X. Xin and G. Fu, *J. Mater. Chem. C*, 2025, **13**, 9474–9482.
38 L. Li, S.-H. Li, Z.-Y. Li, N.-N. Zhang, Y.-T. Yu, J.-G. Zeng and Y. Hua, *Coord. Chem. Rev.*, 2024, **518**, 216064.
39 M. Kanagaraj, A. Vijayaprabhakaran and M. Kathiresan, *Polym. Chem.*, 2025, **16**, 3995–4008.
40 M. Boundor, B. Bielska, N. Katir, N. Wrońska, K. Lisowska, M. Bryszewska, K. Miłowska and A. El Kadib, *ACS Appl. Polym. Mater.*, 2023, **5**, 9952–9963.
41 Y. Chang, S. Wang, J. Chen, Z. Xu, Q. Shi, Y. Mao, Y. Gai, Z. Long and G. Chen, *Green Chem.*, 2024, **26**, 10876–10885.
42 E. Grignon, J. T. Liu, Y. F. Tan, Y. Cao, A. Aspuru-Guzik and D. S. Seferos, *J. Am. Chem. Soc.*, 2025, **147**, 5071–5079.
43 Z. Xu, K. Liu, S. Wang, Y. Chang, J. Chen, S. Wang, C. Meng, Z. Long, Z. Qin and G. Chen, *ACS Appl. Polym. Mater.*, 2024, **6**, 701–711.
44 G. Xu, G.-C. Guo, M.-S. Wang, Z.-J. Zhang, W.-T. Chen and J.-S. Huang, *Angew. Chem., Int. Ed.*, 2007, **46**, 3249–3251.
45 T. Fiala, L. Ludvíková, D. Heger, J. Švec, T. Slanina, L. Vetráková, M. Babiak, M. Nečas, P. Kulhánek, P. Klán and V. Sindelar, *J. Am. Chem. Soc.*, 2017, **139**, 2597–2603.
46 J. A. McCune, M. F. Kuehnel, E. Reisner and O. A. Scherman, *Chem*, 2020, **6**, 1819–1830.
47 Y. Shi, M. A. Soto, Z. Li and M. J. MacLachlan, *New J. Chem.*, 2024, **48**, 10588–10592.

48 C. Herrmann, G. C. Solomon and M. A. Ratner, *J. Am. Chem. Soc.*, 2010, **132**, 3682–3684.
49 G. Spagnol, K. Shiraishi, S. Rajca and A. Rajca, *Chem. Commun.*, 2005, 5047–5049.
50 J. Peon, X. Tan, J. D. Hoerner, C. Xia, Y. F. Luk and B. Kohler, *J. Phys. Chem. A*, 2001, **105**, 5768–5777.
51 T. J. Trivedi, J. H. Lee, H. J. Lee, Y. K. Jeong and J. W. Choi, *Green Chem.*, 2016, **18**, 2834–2842.
52 S. Lu, X. Hu, B. Xu, C. Bai, T. Wang, T. Ma and Y. Song, *Food Hydrocoll.*, 2024, **151**, 109799.
53 T. M. Bockman and J. K. Kochi, *J. Org. Chem.*, 1990, **55**, 4127–4135.
54 A. S. Hopkins, A. Ledwith and M. F. Stam, *J. Chem. Soc. D*, 1970, 494–495.
55 P. Hyde and A. Ledwith, *J. Chem. Soc., Perkin Trans. 2*, 1974, 1768–1772.
56 J. Onodera, X. Zhang, T. Tanaka, R. Nakada, M. Okazaki, N. Tarutani, K. Katagiri and K. Maeda, *ACS Catal.*, 2026, **16**, 3368–3379.
57 M. R. Geraskina, A. S. Dutton, M. J. Juetten, S. A. Wood and A. H. Winter, *Angew. Chem., Int. Ed.*, 2017, **56**, 9435–9439.
58 T. Sagara and H. Tahara, *Chem. Rec.*, 2021, **21**, 2375–2388.
59 G. Cooke, H. Augier de Cremiers, F. M. A. Duclairoir, M. Gray, P. Vaqueiro, A. V. Powell, G. Rosair and V. M. Rotello, *Tetrahedron Lett.*, 2001, **42**, 5089–5091.
60 Y. Wang, M. Frasconi, W.-G. Liu, Z. Liu, A. A. Sarjeant, M. S. Nassar, Y. Y. Botros, W. A. I. Goddard and J. F. Stoddart, *J. Am. Chem. Soc.*, 2015, **137**, 876–885.
61 R. Ghahremani, W. Dean, N. Sinclair, X. Shen, N. Starvaggi, I. Alfurayj, C. Burda, E. Pentzer, J. Wainright, R. Savinell and B. Gurkan, *ACS Appl. Mater. Interfaces*, 2023, **15**, 1148–1156.
62 Y. Neagari, M. A. Soto, Y. Zhang, Z. Li, C. A. Michal and M. J. MacLachlan, *Mater. Horiz.*, 2025, **12**, 10184–10193.
63 B. Odell, M. V. Reddington, A. M. Z. Slawin, N. Spencer, J. F. Stoddart and D. J. Williams, *Angew. Chem., Int. Ed. Engl.*, 1988, **27**, 1547–1550.
64 I. R. Fernando, M. Frasconi, Y. Wu, W.-G. Liu, M. R. Wasielewski, W. A. I. Goddard and J. F. Stoddart, *J. Am. Chem. Soc.*, 2016, **138**, 10214–10225.
65 A. Trabolsi, N. Khashab, A. C. Fahrenbach, D. C. Friedman, M. T. Colvin, K. K. Cotí, D. Benítez, E. Tkatchouk, J.-C. Olsen, M. E. Belowich, R. Carmielli, H. A. Khatib, W. A. Goddard, M. R. Wasielewski and J. F. Stoddart, *Nat. Chem.*, 2010, **2**, 42–49.
66 Z. Zhu, A. C. Fahrenbach, H. Li, J. C. Barnes, Z. Liu, S. M. Dyar, H. Zhang, J. Lei, R. Carmieli, A. A. Sarjeant, C. L. Stern, M. R. Wasielewski and J. F. Stoddart, *J. Am. Chem. Soc.*, 2012, **134**, 11709–11720.
67 A. C. Fahrenbach, Z. Zhu, D. Cao, W.-G. Liu, H. Li, S. K. Dey, S. Basu, A. Trabolsi, Y. Y. Botros, W. A. I. Goddard and J. F. Stoddart, *J. Am. Chem. Soc.*, 2012, **134**, 16275–16288.
68 C. K. Lee, J. P. Violi, W. A. Donald, J. F. Stoddart and D. J. Kim, *Nat. Commun.*, 2025, **16**, 5922.
69 J. S. W. Seale, S. Sharma, C. K. Lee, H. Han, T. Jaynes, E. W. Roth, S. Shafie, Y. Qiu, L. Malaisrie, M. I. Bardot, L. Zhang, Y.-K. Xing, D. J. Kim, S. I. Stupp, R. D. Astumian, E. A. Scott, W. R. Dichtel and J. F. Stoddart, *Angew. Chem., Int. Ed.*, 2025, **64**, e202512899.